

## Preparation of ITO Films with Smooth Surface and Low Resistivity Using Reactive Ion-Beam Sputtering

Satoshi IWATSUBO

Toyama Industrial Technology Center, 150 Futagami, Toyama, Toyama 933-0981

Fax: 81-76-21-2402, e-mail: iwatsubo@itc.pref.toyama.jp

ITO films were prepared by reactive ion-beam sputtering of four ways as a parameter of introduction ways of oxygen gas and positions of substrates. Oxygen gas to react was introduced near the substrates ( $Ar+[O_2]$ ) or into the ion source ( $Ar+O_2$ ). The films prepared by both ways are bombarded by recoiled argon from the target. For  $Ar+[O_2]$ , the films are exposed to the absorptive oxygen. For  $Ar+O_2$ , the films are bombarded by oxygen recoiled from the target in addition to the adsorptive oxygen. The energies of the recoiled argon and oxygen arriving at the substrates were estimated from the Monte-Carlo simulation. Their values strongly depended on the positions. The dependence of electrical and optical properties and surface morphologies on the ratio in flowing rate of  $O_2$  gas to total rates of Ar and  $O_2$  gases,  $R_{O_2}$  and on the positions,  $\theta_s$  has been investigated. The films with the low resistivity of  $6.3 \times 10^{-4} \Omega \text{cm}$ , transmittance higher than 90 % and smooth surface were prepared by reactive sputtering for  $Ar+[O_2]$ . It was found that the energy of recoiled ions of the sputtering was the important parameters to prepare the ITO films with smooth surface and low resistivity.

Key words: ITO, ion beam, sputtering, thin film, oxygen, argon, roughness

### 1. INTRODUCTION

Transparent conductive films, represented by  $\text{In}_2\text{O}_3$ : Sn (ITO) and ZnO are widely used as electrodes for flat panel displays, solar cells and electro luminescence (EL) devices [1,2]. So far, ITO films are prepared by various methods such as chemical vapor deposition (CVD), evaporation, sputtering. Among these methods, ITO films with low resistivity are frequently deposited by rf magnetron sputtering [3], dc magnetron sputtering under low sputtering voltage [4] and FTS (Facing Target System) of plasma free process [5]. Recent technology requires a preparation method of the films with high qualities in low resistivity and smooth surface at low temperature. For organic EL device, an increase of surface roughness is known to deteriorate color quality and to reduce lifetime of the device [6-8]. Therefore, the surface roughness of the films should be decreased to achieve high performance. However, the relationship between surface morphology of the films and sputtering conditions at the films has not been discussed in detail. The sputtering conditions of energies of sputtered atoms and recoiled ions from target are very important for reactive sputtering using oxygen and argon gases. For conventional plasma sputtering, substrates are placed near the plasma in the apparatus, so that the films are always bombarded by the ions from the plasma. It is difficult to clear

their bombarding effects on the surface morphology and the properties of the prepared films.

On the other hand, ion-beam sputtering has the advantage that substrates are separated far from the plasma, so that adsorptive atoms, ionized ions in the plasma and ions recoiled from the target are experimentally separated [9,10]. In this study, the ITO films were prepared by reactive ion-beam sputtering, and the dependence of the properties and surface morphologies on the ratio in flowing rate of  $O_2$  gas to total flow rate of Ar and  $O_2$  gases,  $R_{O_2}$  and on the positions of substrates,  $\theta_s$  has been investigated.

### 2. EXPERIMENTAL PROCEDURE

Figure 1 shows the schematic illustration of the ion-beam sputtering apparatus used in this study and the two ways to introduce oxygen gas. Kaufman-type ion source and ITO ( $\text{In}_{35}\text{Sn}_{5}\text{O}_{60}$ ) target were used. The two substrates were set at the position parallel to the target plane and at the position tilted to  $45^\circ$ . The ITO films were prepared on silica glass substrates. The residual gas pressure in the chamber was lower than  $6.0 \times 10^{-5}$  Pa. Argon gas of 99.999% in purity for sputtering was introduced into the ion source at flowing rate of 2 sccm, so that argon pressure was as high as 3.6 mPa. Oxygen gas was introduced by the two ways into the chamber ( $Ar+[O_2]$ ) and into the ion source ( $Ar+O_2$ ), as shown Fig. 1. The flowing rate of

oxygen was varied in the range between 0.125 and 16 sccm. The total gas pressure in the chamber was in the range between  $5.3 \times 10^{-3}$  and  $4.1 \times 10^{-2}$  Pa. The mean free path of the ions of argon and oxygen at the flowing rate of 16 sccm was longer than the distance of target and substrates. So, the recoiled ions from the target directly arrive at the substrates. The sputtering voltage and current were fixed at 1200 V and 30 mA, respectively. Film thickness was 400 nm. The temperature of the substrate holder was approximately up to 130°C. The composition of the films was analyzed by an X-ray photoelectron spectroscopy (XPS). The morphology of the films was observed by an atomic force microscope (AFM). The resistivity  $\rho$  was measured using by a four probe method. The optical transmission spectra of the films were measured by a spectroscope in the wave range from 300 to 2100 nm.

Introduction way:

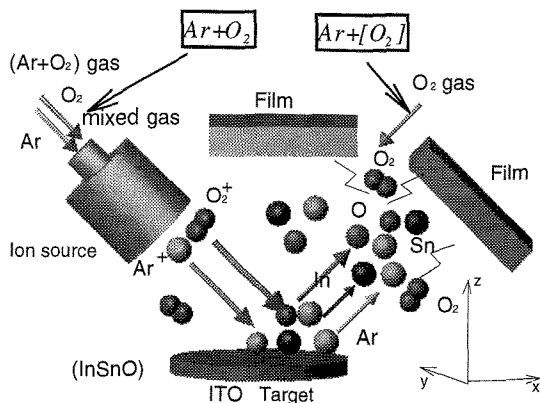


Fig. 1. Schematic illustration of ion-beam sputtering apparatus used in this study and the ways of introduce gases.

### 3. RESULTS AND DISCUSSION

#### 3.1 Simulation of recoiled argon and oxygen

It is known that energy and amount of ions recoiled from target are closely related to mass numbers of target atoms and sputtering ions. The mass numbers of indium, tin, argon and oxygen are 114.8, 118.7, 39.9 and 16, respectively. The mass numbers of argon and oxygen as sputtering gas are much smaller than that of the target elements. Therefore, there is a high possibility that the films are bombarded by a large amount of the recoiled argon and the recoiled oxygen. So, their energies and angular distributions of the recoiled ions and sputtered atoms were estimated from Monte-Carlo simulation TRIM [11]. The calculations are based on a direct Monte-Carlo method applied to an amorphous ITO target. Figure 2 shows the schematic layout of the apparatus and the angular distribution in energy of the recoiled argon. The angle of the substrates,  $\theta_s$  is defined in Fig. 2. The incident angle of the sputtering ion-beam is equal to 135°. The substrates are set on

the holders at  $\theta_s$  of 45° ( $\theta_{45}$ ) or 90° ( $\theta_{90}$ ). The simulation was carried out at acceleration voltage of 1200 V and 100000 events. The small dot in the figure corresponds to an argon atom. The length from the center of the target to the dot indicates the energy. The angle to the dot indicates the direction projected in the plane included the points of the ion source, the target and the substrates. In Fig. 2, a large amount of argon is reflected from the target to the substrates. The substrate at  $\theta_{45}$  was bombarded by recoiled argon with very high energy up to 800 eV.

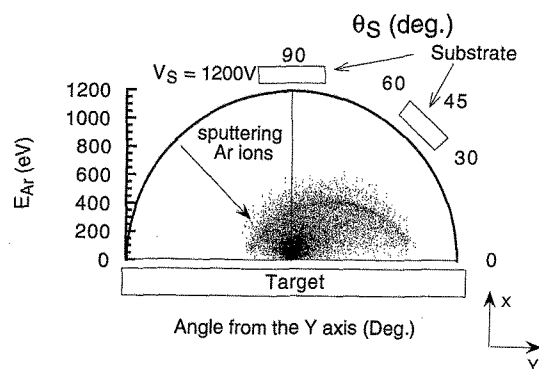


Fig. 2. Angular distribution and energy of recoiled argon.

The average energy  $\langle E_{Ar} \rangle$  of argon reaching the substrate at  $\theta_{45}$  was 280 eV. Similarly, the average energy of the recoiled oxygen  $\langle E_O \rangle$  was 202 eV. At  $\theta_{90}$ ,  $\langle E_{Ar} \rangle$  and  $\langle E_O \rangle$  were 138 eV and 131 eV, respectively. On the other hand, the sputtered atoms of indium, tin and oxygen did not show such angular dependence of energy. Their average energies were in the range between 20 and 53 eV. These results indicate that the energies of recoiled ions generated by ion-beam sputtering strongly depend on the position of substrates.

For reactive ion-beam sputtering, two ways to introduce oxygen gas are considered. Oxygen gas to react is introduced near the substrates ( $Ar+[O_2]$ ) and into the ion source ( $Ar+O_2$ ). The ions from the ion source frequently reflect at the target and become recoiled ions. So, the films prepared by both ways are bombarded by recoiled ions of argon as a sputtering gas. For  $Ar+[O_2]$ , the films are exposed to the absorptive oxygen with the thermal energy. On the other hand, for  $Ar+O_2$ , the films are bombarded by oxygen recoiled from the target in addition to the adsorptive oxygen. Therefore, the ITO films are prepared by the reactive ion-beam sputtering of the four ways under the four sputtering conditions as a parameter of the ways to introduce oxygen gas ( $Ar+[O_2]$ ,  $Ar+O_2$ ) and the position of the substrates ( $\theta_s$ ), as shown Table I.

Table I

Position of Substrate	Way of Introduce gases	Arriving particles (+ sputtered atoms)
(1) $\theta_{45}$	$Ar+[O_2]$	recoiled argon (280 eV) and adsorptive oxygen
(2) $\theta_{45}$	$Ar+O_2$	recoiled argon (280 eV) and recoiled oxygen (202 eV)
(3) $\theta_{90}$	$Ar+[O_2]$	recoiled argon (130 eV) and adsorptive oxygen
(4) $\theta_{90}$	$Ar+O_2$	recoiled argon (130 eV) and recoiled oxygen (131 eV)

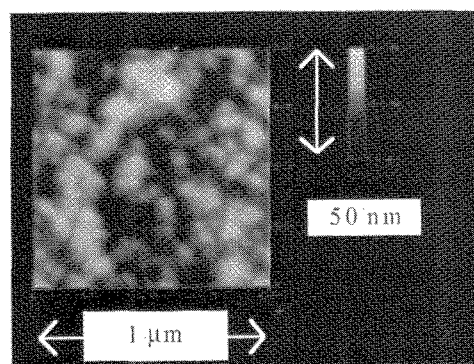
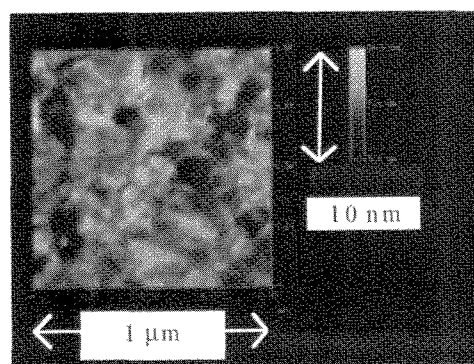
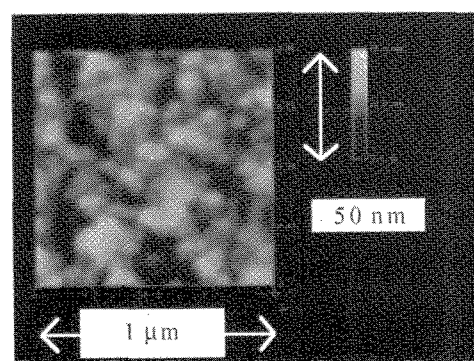
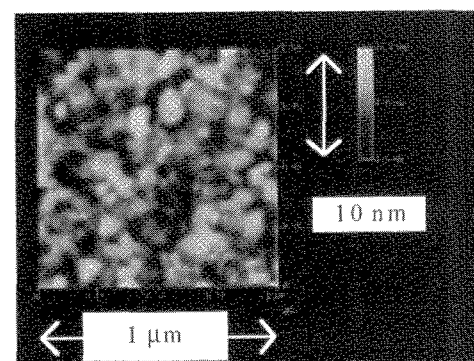
### 3.2 Experimental results

The contents of indium and tin of the films analyzed by XPS were nearly equal to 35 and 5 at.% of the target, respectively. The contents did not depend on  $\theta_s$ . The oxygen content of the films increased in the range between 57 and 59 at.%, as  $R_{O_2}$  increased.

Figures 3 and 4 show the typical AFM images of the ITO films prepared at  $R_{O_2}$  of 0.67 for  $Ar+[O_2]$  and at  $R_{O_2}$  of 0.20 for  $Ar+O_2$ , respectively. The scanning area of the images is  $1 \times 1 \mu m^2$ . (a) and (b) in their figures are surface images at  $\theta_{45}$  and  $\theta_{90}$ , respectively. The maximum scales of height for (a) and (b) are 50 nm and 10 nm. The average roughness parameter  $R_a$  and the height parameter  $R_z$  of the films were estimated from the images. The values of  $R_a$  and  $R_z$  of the films were very different between them.  $R_a$  of the films bombarded by the recoiled argon at  $\theta_{45}$  was in the range between 4.2 and 5.6 nm.  $R_a$  of the films at  $\theta_{90}$  was smaller than that at  $\theta_{45}$ .  $R_a$  of the films at  $\theta_{90}$  for  $Ar+[O_2]$  took the minimum value of 0.92 nm. The spherical grains except the films at  $\theta_{90}$  for  $Ar+[O_2]$  appeared. These results indicate that the bombardment by the recoiled ions with the energy higher than 200 eV roughens the film surface by re-sputtering and may form the spherical grains due to the promotion of crystallization.

Figure 5 shows the  $R_{O_2}$  dependence of resistivity  $\rho$  for  $Ar+[O_2]$ .  $\rho$  of films took the minimum values at  $R_{O_2}$  of 0.11 at  $\theta_{45}$  and 0.67 at  $\theta_{90}$ , respectively.  $\rho$  was the lowest value of  $6.5 \times 10^{-4} \Omega cm$  at  $\theta_{45}$ . This result indicates that the bombardment by the recoiled argon increased  $\rho$ .

Figure 6 shows the  $R_{O_2}$  dependence of resistivity  $\rho$  for  $Ar+O_2$ .  $\rho$  of the films took the minimum values of  $6.3 \times 10^{-4} \Omega cm$  at  $R_{O_2}$  of 0.33 at  $\theta_{45}$  and 0.20 at  $\theta_{90}$ , respectively.  $\rho$  for  $Ar+O_2$  drastically increased at  $R_{O_2}$  above 0.33 at  $\theta_{45}$  and 0.67 at  $\theta_{90}$ . The changes for  $Ar+O_2$  were larger than that for  $Ar+[O_2]$ . From the increase of oxygen content with an increase of  $R_{O_2}$ , the recoiled oxygen with the energy higher than 130 eV promotes the oxidation of the films, so that the density of carrier electrons in the films may abruptly decreased.

(a)  $\theta_{45}$  ( $R_a = 4.20$  nm,  $R_z = 36.4$  nm)(b)  $\theta_{90}$  ( $R_a = 0.92$  nm,  $R_z = 10.6$  nm)Fig. 3. AFM images of ITO films at  $R_{O_2}$  of 0.67 for  $Ar+[O_2]$ .(a)  $\theta_{45}$  ( $R_a = 5.60$  nm,  $R_z = 53.5$  nm)(b)  $\theta_{90}$  ( $R_a = 1.38$  nm,  $R_z = 12.4$  nm)Fig. 4. AFM images of ITO films at  $R_{O_2}$  of 0.20 for  $Ar+O_2$ .

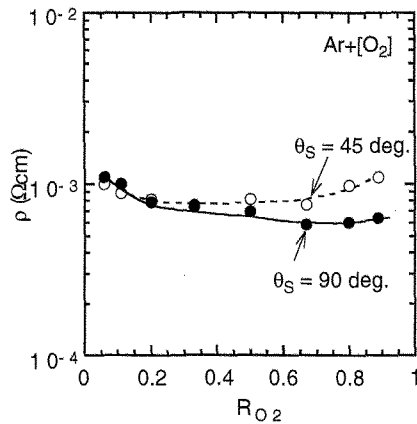


Fig. 5.  $R_{O_2}$  dependence of resistivity  $\rho$  for  $Ar+[O_2]$ .

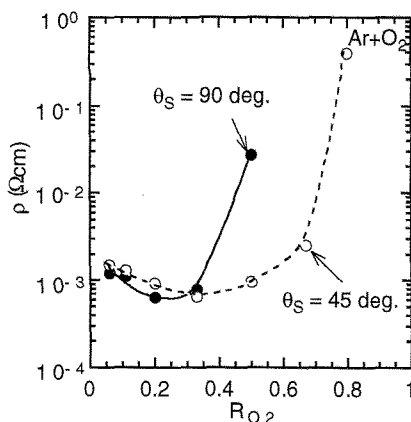


Fig. 6.  $R_{O_2}$  dependence of  $\rho$  for  $Ar+O_2$ .

Figure 7 shows the typical transmittance  $T$  spectra of the ITO films with low  $\rho$  as a parameter of  $R_{O_2}$  at  $\theta_{45}$  and  $\theta_{90}$  for  $Ar+[O_2]$ . Both of  $T$  increased with an increase of  $R_{O_2}$ .  $T$  at  $\theta_{90}$  is higher than that at  $\theta_{45}$ . The changes of  $T$  for  $Ar+O_2$  were as same as one for  $Ar+[O_2]$ . These results indicate that it is necessary to prepare the films with smooth surface to increase  $T$  of the films. The reactive ion-beam sputtering at  $\theta_{90}$  for  $Ar+[O_2]$  is the best condition to prepare the good ITO films with smooth surface and high  $T$  among the four ways.

#### 4. CONCLUSION

The energies and distributions of the recoiled argon and the recoiled oxygen of the reactive ion-beam sputtering were estimated. The positions of the substrates related to the energy of recoiled ions from the target. The ways of introduce oxygen gas related to the generation of adsorptive oxygen and recoiled oxygen. Their parameters to prepare the films using the reactive ion-beam sputtering were as important as the gas flow. The bombardment of the recoiled oxygen changed the optimum conditions of the gas flow to prepare the films with low resistivity. The bombardment by the recoiled ions with the energy

higher than 130 eV increased the surface roughness of the films. It was found that the ITO films with smooth surface and low resistivity were prepared under the sputtering condition that the energy of the recoiled ions was smaller than 200 eV.

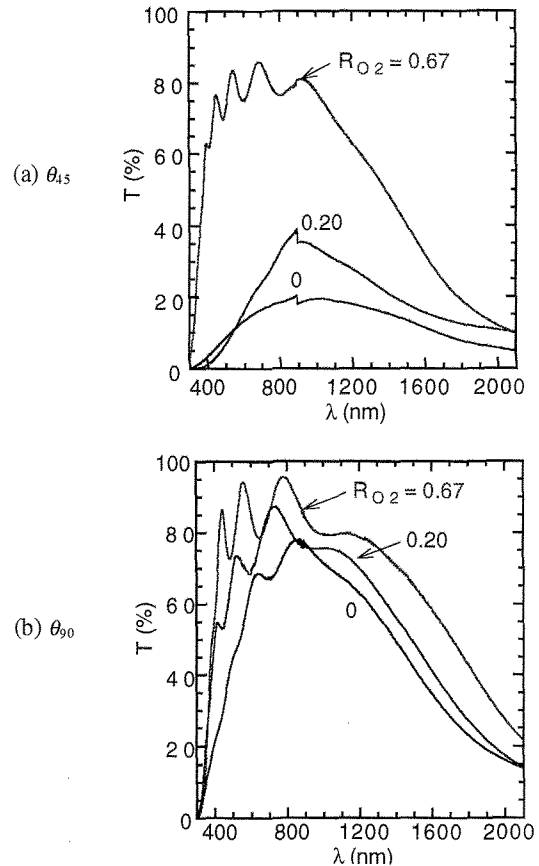


Fig. 7. Transmittance  $T$  spectra of ITO films with low  $\rho$  as a parameter of  $R_{O_2}$  at  $\theta_{45}$  and  $\theta_{90}$  for  $Ar+[O_2]$ .

#### REFERENCES

- [1] K. L. Chopra, S. Major and D. K. Pandya, *Thin Solid Films*, **102**, 1-46 (1983)
- [2] I. Hamberg and C. G. Granqvist, *J. Appl. Phys.*, **60**, R123-R160 (1986)
- [3] K. Sreenivas, T. S. Rao and A. Mansingh, *J. Appl. Phys.*, **57**, 384-392 (1985)
- [4] R. Ohki and Y. Hoshi, *Technical Report of IEICE (CPM99)*, **99**, 27-31, (1999) in Japanese
- [5] Y. Hoshi, *Technical Report of IEICE (CPM98)*, **98**, 15-21, (1998) in Japanese
- [6] Yoon-Heung Tak, Ki-Beom Kim, Hyung-Guen Park, Kwang-Ho Lee, Jong-Ram Lee, *Thin Solid Films*, **411**, 12-16 (2002)
- [7] C. Liu, T. Matsutani, T. Asanuma, K. Murai, M. Kikuchi, E. Alves and M. Reis, *J. Appl. Phys.*, **93**, 2262-2266 (2003)
- [8] Y. Shigesato, R. Koshi-ishi, T. Kawashima, J. Ohsako, *Vacuum*, **59**, 614-621, (2000)
- [9] S. Iwatsubo and M. Naoe, *Vacuum*, **66**, 251-256, (2002)
- [10] S. Iwatsubo, *Trans. MRS-J*, **29**, 1483-1486 (2004)
- [11] J. P. Biersack, W. Eckstein, *Appl. Phys., A*, **34**, 73-94 (1984)